Same-Sign Diboson Signature from Supersymmetry Models with Light Higgsinos at the LHC

Howard Baer,[1] Vernon Barger,[2] Peisi Huang,[2] Dan Mickelson,[1] Azar Mustafayev,[3] Warintorn Sreethawong,[4] and Xerxes Tata[3]

[1]*Department of Physics and Astronomy, University of Oklahoma, Norman, Oklahoma 73019, USA*
[2]*Department of Physics, University of Wisconsin, Madison, Wisconsin 53706, USA*
[3]*Department of Physics and Astronomy, University of Hawaii, Honolulu, Hawaii 96822, USA*
[4]*School of Physics, Suranaree University of Technology, Nakhon Ratchasima 30000, Thailand*

(Received 25 February 2013; published 9 April 2013)

In supersymmetric models with light Higgsinos (which are motivated by electroweak naturalness arguments), the direct production of Higgsino pairs may be difficult to search for at the LHC due to the low visible energy release from their decays. However, the wino pair production reaction $\tilde{W}_2^{\pm}\tilde{Z}_4 \to (W^{\pm}\tilde{Z}_{1,2}) + (W^{\pm}\tilde{W}_1^{\mp})$ also occurs at substantial rates and leads to final states including equally opposite-sign and same-sign diboson production. We propose a novel search channel for LHC14 based on the same-sign diboson plus missing E_T final state which contains only modest jet activity. Assuming gaugino mass unification, and an integrated luminosity $\gtrsim 100$ fb^{-1}, this search channel provides a reach for supersymmetry well beyond that from usual gluino pair production.

DOI: 10.1103/PhysRevLett.110.151801 PACS numbers: 12.60.Jv, 13.85.Rm, 14.80.Ly

The recent discovery of a Higgs-like resonance at $m_h \sim 125$ GeV by the Atlas and CMS Collaborations [1,2] completes the identification of all the states in the standard model (SM). However, the existence of fundamental scalars in the SM is problematic in that they lead to gauge instability and fine-tuning issues. Supersymmetric (SUSY) theories stabilize the scalar sector due to a fermion-boson symmetry, thus providing a solution to the gauge hierarchy problem [3]. In fact, the measured Higgs boson mass $m_h \simeq 125$ GeV falls squarely within the narrow range predicted [4] by the minimal supersymmetric standard model (MSSM); this may be interpreted as indirect support for weak scale SUSY. In contrast, the associated superparticle states have failed to be identified at LHC, leading the Atlas and CMS Collaborations [5,6] to place limits of $m_{\tilde{g}} \gtrsim 1.4$ TeV (for $m_{\tilde{g}} \simeq m_{\tilde{q}}$) and $m_{\tilde{g}} \gtrsim 0.9$ TeV (for $m_{\tilde{g}} \ll m_{\tilde{q}}$) within the popular mSUGRA/CMSSM model [7].

In many SUSY models used for phenomenological analyses, the Higgsino mass parameter $|\mu|$ is larger than the gaugino mass parameters $|M_{1,2}|$. In the alternative case where $|\mu| \ll |M_{1,2}|$, the lighter electroweak chargino $\tilde{W}_1$ and the lighter neutralinos $\tilde{Z}_{1,2}$ are Higgsino-like, while (assuming $|M_2| > |M_1|$) the heavier chargino and the heaviest neutralino $\tilde{Z}_4$ is winolike, and $\tilde{Z}_3$ is binolike. Electroweak $\tilde{W}_2\tilde{Z}_4$ production, which occurs with $SU(2)$ gauge strength, then leads to a novel $W^{\pm}W^{\pm} + \not{E}_T$ signature via the process shown in Fig. 1. We examine prospects for observing this signal in the 14 TeV run of the CERN LHC.

Models with light Higgsinos have a number of theoretical advantages, and have recently received considerable attention. To understand why, we note that the minimization condition for the Higgs scalar potential leads to the well-known (tree-level) relation,

$$\frac{M_Z^2}{2} = \frac{m_{H_d}^2 - m_{H_u}^2 \tan^2\beta}{(\tan^2\beta - 1)} - \mu^2 \simeq -m_{H_u}^2 - \mu^2, \qquad (1)$$

where $m_{H_u}^2$ and $m_{H_d}^2$ are the tree-level mass squared parameters of the two Higgs doublets that are required to give masses to up- and down-type quarks, and $\tan\beta$ is the ratio of their vacuum expectation values. The value of M_Z that is obtained from (1) is natural if the three terms on the right-hand side each have a magnitude of the same order as M_Z^2, implying $\mu^2/(M_Z^2/2)$ is limited from above by the extent of fine-tuning one is willing to tolerate. The lack of a chargino signal at the LEP2 collider requires $|\mu| \gtrsim 103.5$ GeV [8], so that light Higgsino models with low fine-tuning favor $|\mu| \sim 100$–300 GeV (in fact, μ^2 was suggested as a measure of fine-tuning in Ref. [9]). When radiative corrections to (1) are included, masses of other superpartners (most notably third generation squarks) also enter on the right-hand side, and large cancellations may be needed if these have super-TeV masses. Models favoring low values of $|\mu|$ include (i) the hyperbolic branch or focus point region of the minimal supergravity model (mSUGRA or CMSSM)

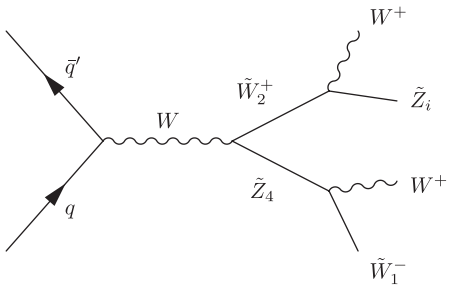

FIG. 1. Diagram depicting same-sign diboson production at LHC in SUSY models with light Higgsinos.

[10] or its nonuniversal Higgs mass extension [11], (ii) models of "natural SUSY" [12–15] which have $\mu \sim$ 100–300 GeV and top and bottom squarks with $m_{\tilde{t}_{1,2}}, m_{\tilde{b}_1} \lesssim$ 500 GeV, and $m_{\tilde{g}} \lesssim 1.5$ TeV, and (iii) radiative natural SUSY (RNS) [16], where again $\mu \sim$ 100–300 GeV and where $m^2_{H_u}$ is driven to small values $\sim -M_Z^2$ via the large top quark Yukawa coupling.

The hyperbolic branch or focus point region of mSUGRA [7] remains viable [17] but suffers high fine-tuning due to large top squark masses. The natural SUSY models as realized within the MSSM also seem to be disfavored because much heavier top squark masses are required to lift m_h up to 125 GeV and to bring the $b \to s\gamma$ branching fraction into accord with measurements [15]. Models of natural SUSY with extra exotic matter which provide additional contributions to m_h would still be allowed [18]. The RNS model allows for top and bottom squarks in the 1–4 TeV range, and with large mixing can accommodate $m_h \simeq 125$ GeV and BF$(b \to s\gamma)$ while maintaining cancellations in (1) at the 3%–10% level.

Another potential advantage of models with light Higgsinos is that, if the lightest supersymmetric particle is Higgsino-like, then it annihilates rapidly in the early Universe, thus avoiding cosmological overclosure bounds. In this case, the Higgsino might serve as a co-dark-matter particle along with perhaps the axion [19].

Although the production of charged and neutral Higgsinos may occur at large rates (pb-level cross sections for $\mu \sim 150$ GeV at the LHC), detection of these reactions is very difficult because the mass gaps $m_{\tilde{W}_1} - m_{\tilde{Z}_1}$ and $m_{\tilde{Z}_2} - m_{\tilde{Z}_1}$ are typically small, ~520 GeV, resulting in very low visible energy release from $\tilde{W}_1$ and $\tilde{Z}_2$ decays. Thus, Higgsino pair production events are expected to be buried beneath SM backgrounds [20]. We examine instead signals from the heavier gauginolike states focusing on the winolike states $\tilde{W}_2$ and $\tilde{Z}_4$, whose production cross sections will be fixed by essentially just the wino mass parameter M_2 if first generation squarks are heavy.

As an illustration, we show sparticle production cross sections for a model line from the RNS model, which can be generated from the two-extra-parameter nonuniversal Higgs model (NUHM2) [21] with parameters

$$m_0, m_{1/2}, A_0, \tan\beta, \mu, \text{ and } m_A. \quad (2)$$

The independent grand unified theory scale parameters $m^2_{H_u}$ and $m^2_{H_d}$ have been traded for convenience for the weak scale parameters μ and m_A. We take $m_0 = 5$ TeV, $A_0 = -1.6m_0$, $\tan\beta = 15$, $\mu = 150$ GeV, $m_A = 1$ TeV, and allow $m_{1/2}$ to vary between 300 and 1000 GeV. The large negative A_0 value allows $m_h \sim 125$ GeV [22] and at the same time limits the cancellation between the terms in (1) to no better than 3.5%. We use ISAJET [23] for spectrum generation, branching fractions, and also later for signal event generation.

The cross sections for various electroweak-ino pair production are shown versus $m_{1/2}$ in Fig. 2 for pp collisions at $\sqrt{s} = 14$ TeV, where we have used PROSPINO [24] to obtain results at next-to-leading-order in QCD. The difficult-to-detect $\tilde{W}_1^+\tilde{W}_1^-$, $\tilde{W}_1\tilde{Z}_1$, and $\tilde{Z}_1\tilde{Z}_2$ Higgsino processes dominate sparticle production with a cross section $\sigma \sim (24) \times 10^3$ fb. The corresponding curves are nearly flat with $m_{1/2}$ variation since μ is fixed at 150 GeV. The charged and neutral winolike states $\tilde{W}_2$ and $\tilde{Z}_4$ are mainly produced via $\tilde{W}_2\tilde{Z}_4$ and $\tilde{W}_2^+\tilde{W}_2^-$ reactions with cross sections that begin at ~1000 fb but fall slowly with increasing $m_{1/2}$ because their masses increase with $m_{1/2}$ (since $m_{\tilde{W}_2} \simeq m_{\tilde{Z}_4} \simeq M_2 \sim 0.8m_{1/2}$). Cross sections for mixed gaugino-Higgsino production reactions such as $\tilde{W}_2\tilde{Z}_2$, $\tilde{W}_1\tilde{Z}_3$, etc. fall more rapidly with $m_{1/2}$ and become subdominant. The gluino pair production cross section ("+" symbols on the red curve) starts at ~1000 fb, but drops rapidly as $m_{1/2}$ (alternatively, $m_{\tilde{g}} \simeq 2.4m_{1/2}$) increases.

To understand the final states, we show in Fig. 3 the dominant $\tilde{W}_2$ branching fractions versus $m_{1/2}$ along the same model line. Here, we see that $\tilde{W}_2^+ \to \tilde{W}_1^+ Z$ and $\tilde{Z}_2 W^+$ at about 25% each while $\tilde{W}_2^+ \to \tilde{Z}_1 W^+$ is increasing with $m_{1/2}$ to also approach ~25%.

In Fig. 4, we show the $\tilde{Z}_4$ branching fraction versus $m_{1/2}$, and here find $\tilde{Z}_4 \to \tilde{W}_1^+ W^- + \tilde{W}_1^- W^+$ occurring at ~50%, followed by $\tilde{Z}_4 \to \tilde{Z}_2 Z$ and $\tilde{Z}_1 h$ occurring at the ~15%–20% level; several other subdominant decay modes are also shown.

Combining the $\tilde{W}_2^\pm \tilde{Z}_4$ production reaction with decay modes, the following potentially interesting signatures emerge: $\tilde{W}_2^\pm \tilde{Z}_4 \to (W^+W^-, WZ, ZZ, \text{ and } W^\pm W^\pm) + \not{E}_T$. (The W^+W^-, WZ, and ZZ plus $\not{E}_T$ signals also arise from chargino and neutralino production in models such as mSUGRA/CMSSM.) The W^+W^- signal will likely be buried beneath prodigious SM backgrounds from W^+W^- and $t\bar{t}$ production, while the ZZ signal is likely to be rate

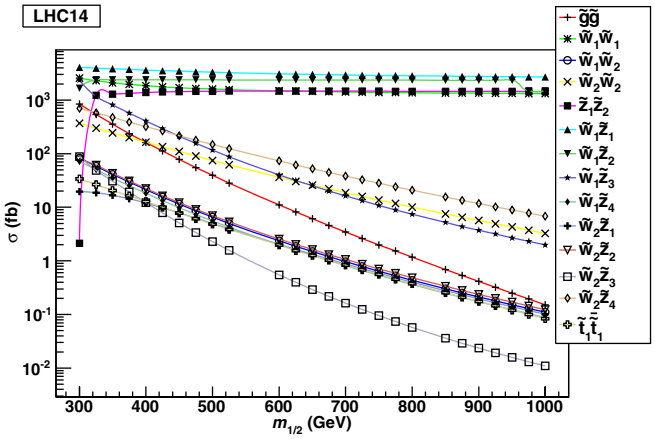

FIG. 2 (color online). Plot of various sparticle pair production cross sections from the RNS model line at LHC with $\sqrt{s} =$ 14 TeV.

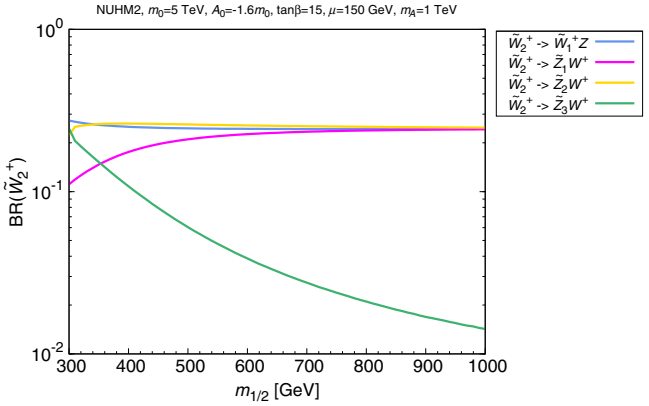

FIG. 3 (color online). Branching fractions of $\tilde{W}_2$ along the RNS model line.

limited at least in the golden four lepton mode. There may also exist some limited LHC14 reach for the $WZ \to 3\ell$ signal as in Ref. [25]. However, same-sign (SS) diboson production—$W^\pm W^\pm + \not{E}_T$—is a novel signature, characteristic of the light Higgsino scenario. Assuming leptonic decays of the W bosons, we expect events with SS dileptons $+\not{E}_T$ accompanied by modest levels of hadronic activity arising from initial state QCD radiation and from hadronic decays of $\tilde{W}_1$ or $\tilde{Z}_2$ where the usually soft decay products might become boosted to create a jet. The SS dilepton signal emerging from wino-pair production is quite distinct from that expected from gluino pair production [26] since in the latter case several very high p_T jets and large $\not{E}_T$ are also expected.

The SM physics backgrounds to the SS diboson signal come from $uu \to W^+W^+dd$ or $dd \to W^-W^-uu$ production, with a cross section ~350 fb. These events will be characterized by high rapidity (forward) jets and rather low $\not{E}_T$. $W^\pm W^\pm$ pairs may also occur via two overlapping events; such events will mainly have low p_T W's and possibly distinct production vertices. Double parton scattering will also lead to SS diboson events, at a rate somewhat lower than the $qq \to W^\pm W^\pm q'q'$ process [27].

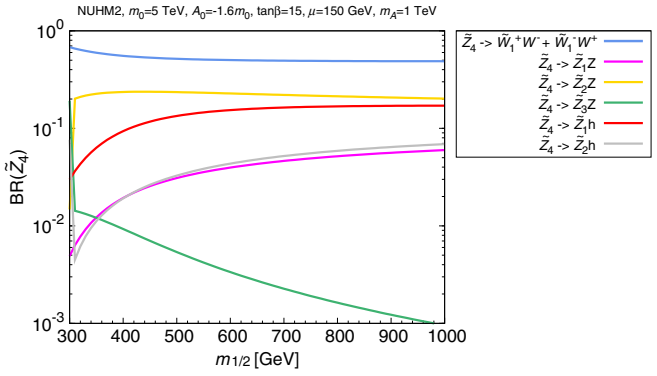

FIG. 4 (color online). Branching fractions of $\tilde{Z}_4$ along the RNS model line.

Additional physics backgrounds come from $t\bar{t}$ production where a lepton from a daughter b is nonisolated, from $t\bar{t}W$ production, and $4t$ production. SM processes such as $WZ \to 3\ell$ and $t\bar{t}Z \to 3\ell$ production, where one lepton is missed, constitute reducible backgrounds to the signal.

To estimate background, we employ a toy detector simulation with calorimeter cell size $\Delta\eta \times \Delta\phi = 0.05 \times 0.05$ and $-5 < \eta < 5$. The hadronic calorimetry energy resolution is taken to be $80\%/\sqrt{E} \oplus 3\%$ for $|\eta| < 2.6$ and the forward calorimetry is $100\%/\sqrt{E} \oplus 5\%$ for $|\eta| > 2.6$, where the two terms are combined in quadrature. The electromagnetic calorimetry energy resolution is assumed to be $3\%/\sqrt{E} \oplus 0.5\%$. In all these, E is the energy in GeV units. We use the cone-type ISAJET [23] jet-finding algorithm to group the hadronic final states into jets. Jets and isolated leptons are defined as follows. (i) Jets are hadronic clusters with $|\eta| < 3.0$, $R \equiv \sqrt{\Delta\eta^2 + \Delta\phi^2} \leq 0.4$, and $E_T(\text{jet}) > 40$ GeV. (ii) Electrons and muons are considered isolated if they have $|\eta| < 2.5$, $p_T(l) > 10$ GeV, with visible activity within a cone of $\Delta R < 0.2$ about the lepton direction, $\Sigma E_T^{\text{cells}} < \min[5, 0.15 p_T(l)]$ GeV. (iii) We identify hadronic clusters as b jets if they contain a B hadron with $E_T(B) > 15$ GeV, $|\eta(B)| < 3.0$, and $\Delta R(B, \text{jet}) < 0.5$. We assume a tagging efficiency of 60%, and light quark and gluon jets can be mistagged as a b jet with a probability $1/R_b$, with $R_b = 150$ for $E_T \leq 100$ GeV, $R_b = 50$ for $E_T \geq 250$ GeV, and a linear interpolation in between.

We require the following cuts on our signal and background event samples: (i) exactly two isolated same-sign leptons with $p_T(\ell_1) > 20$ GeV and $p_T(\ell_2) > 10$ GeV, and (ii) $n(b\,\text{jets}) = 0$ (to aid in vetoing $t\bar{t}$ background).

At this point the event rate is dominated by WZ and $t\bar{t}$ backgrounds. To reduce these further, we construct the transverse mass of each lepton with $\not{E}_T$ and require $m_T^{\min} \equiv \min[m_T(\ell_1, \not{E}_T), m_T(\ell_2, \not{E}_T)] > 125$ GeV, since the signal gives rise to a continuum distribution, while the background has a kinematic cutoff around $m_T^{\min} \simeq M_W$ (as long as the $\not{E}_T$ dominantly arises from the leptonic decay of a single W). After these cuts, we are unable to generate any background events from $t\bar{t}$ and WZ production, where the 1 event level in our simulation was 0.05 fb and 0.023 fb, respectively. The dominant SM background for large $m_T^{\min}$ then comes from $Wt\bar{t}$ production for which we find (including a QCD k factor $k = 1.18$ extracted from Ref. [28]) a cross section of 0.019 (0.006) fb after the harder cuts, $m_T^{\min} > 125$ (175) GeV, and $\not{E}_T > 200$ GeV that serve to optimize the signal reach for high $m_{1/2}$ values. (We have ignored detector-dependent backgrounds from jet-lepton misidentification in our analysis, but are optimistic that these can be controlled by the $m_T^{\min}$ and $\not{E}_T$ cuts.)

The calculated signal rates after cuts along the RNS model line from just $\tilde{W}_2^\pm \tilde{Z}_4$ and $\tilde{W}_2^\pm \tilde{W}_2^\mp$ production are shown versus $m_{1/2}$ in Fig. 5 where the upper (blue) curves require $m_T^{\min} > 125$ GeV and the lower (orange) curve requires $m_T^{\min} > 175$ GeV. The $\tilde{W}_2\tilde{Z}_4$ and $\tilde{W}_2\tilde{W}_2$ cross

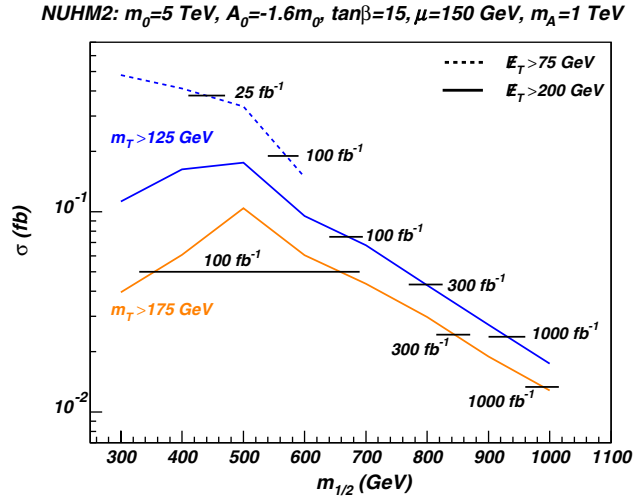

FIG. 5 (color online). Same-sign dilepton cross section (fb) after cuts versus $m_{1/2}$ along the RNS model line from just $\tilde{W}_2^{\pm}\tilde{Z}_4$ and $\tilde{W}_2^{\pm}\tilde{W}_2^{\mp}$ production with $t\bar{t}W$ background and calculated reach for 100, 300, and 1000 fb^{-1}. The upper solid and dashed (blue) curves require $m_T^{\min} > 125$ GeV while the lower solid (orange) curve requires $m_T^{\min} > 175$ GeV. The signal is observable above the horizontal lines.

sections are normalized to those from PROSPINO [24]. For observability with an assumed value of integrated luminosity, we require (1) significance $>5\sigma$, (2) signal to background >0.2, and (3) at least five signal events. The LHC reach for SS diboson events for integrated luminosity values 100, 300, and 1000 fb^{-1} is shown by horizontal lines in Fig. 5 and also in Table I. For just 10 fb^{-1} of integrated luminosity there is no LHC14 reach for SS dibosons, while $\tilde{g}\,\tilde{g}$ production gives a reach of $m_{\tilde{g}} \sim 1.4$ TeV [29]. However, for 100 fb^{-1} the LHC14 reach for SS dibosons extends to $m_{1/2} \sim 680$ GeV corresponding to $m_{\tilde{g}} \sim 1.6$ TeV in a model with gaugino mass unification. The direct search for $\tilde{g}\,\tilde{g}$ gives a projected reach of $m_{\tilde{g}} \sim 1.6$ TeV [30], so already the SS diboson signal offers a comparable reach. For 300 (1000) fb^{-1} of integrated luminosity, we find the LHC14 reach for SS dibosons extends to $m_{1/2} \sim 840$ (1000) GeV, corresponding to a reach in $m_{\tilde{g}}$ of 2.1 and 2.4 TeV. These numbers extend well beyond the LHC14 reach for direct gluino pair production [29].

We emphasize here that the SS diboson signal from SUSY models with light Higgsinos is quite distinct from the usual SS dilepton signal arising from gluino pair production, which is usually accompanied by numerous hard jets and high $\not{E}_T$. For instance, recent CMS searches for SS dileptons from SUSY [31] required the presence of two tagged b jets or large H_T in the events; these cuts reduce or even eliminate our SS diboson signal. Likewise, the cuts $n_j \geq 4$ high p_T jets along with $\not{E}_T > 150$ GeV required by a recent Atlas search for SS dileptons from gluinos [32] would have eliminated much of the SS diboson signal from SUSY with light Higgsinos.

TABLE I. Reach of LHC14 for SUSY assuming various integrated luminosity values. The reach is given for $m_{1/2}$ along the RNS model line, and also for the equivalent reach in $m_{\tilde{g}}$ assuming heavy squarks. The corresponding reach in $m_{\tilde{g}}$ from $\tilde{g}\,\tilde{g}$ searches is also shown for comparison.

Integrated luminosity (fb^{-1})	$m_{1/2}$ (GeV)	$m_{\tilde{g}}$ (TeV)	$m_{\tilde{g}}$ (TeV) [$\tilde{g}\,\tilde{g}$]
10	⋯	⋯	1.4
100	680	1.6	1.6
300	840	2.1	1.8
1000	1000	2.4	2.0

In summary, in SUSY models with light Higgsinos, as motivated by electroweak naturalness considerations, the production of wino pairs gives rise to a novel same-sign diboson plus modest hadronic activity signature. For an integrated luminosity of 100 (1000) fb^{-1}, this SS diboson signal should be observable at LHC14 for wino masses up to 550 (800) GeV. Assuming gaugino mass unification, this extends the LHC SUSY reach well beyond that of conventional searches for gluino pair production in the case where squarks are heavy.

We thank Andre Lessa for discussions. This work was supported in part by the U.S. Department of Energy, Office of High Energy Physics, by Suranaree University of Technology, and by the Higher Education Research Promotion and National Research University Project of Thailand, Office of the Higher Education Commission.

[1] G. Aad *et al.* (ATLAS Collaboration), Phys. Lett. B **710**, 49 (2012).
[2] S. Chatrachyan *et al.* (CMS Collaboration), Phys. Lett. B **710**, 26 (2012).
[3] E. Witten, Nucl. Phys. **B188**, 513 (1981); R. Kaul, Phys. Lett. **109B**, 19 (1982).
[4] M. S. Carena and H. E. Haber, Prog. Part. Nucl. Phys. **50**, 63 (2003).
[5] G. Aad *et al.* (ATLAS Collaboration), Phys. Lett. B **710**, 67 (2012).
[6] S. Chatrchyan *et al.* (CMS Collaboration), Phys. Rev. Lett. **107**, 221804 (2011).
[7] For a review, see, e.g., R. Arnowitt and P. Nath, in *Perspectives on Supersymmetry II*, edited by G. L. Kane (World Scientific, Singapore, 2010), pp. 222–243, and references therein; G. L. Kane, C. Kolda, L. Roszkowski, and J. D. Wells, Phys. Rev. D **49**, 6173 (1994).
[8] Joint LEP 2 Supersymmetry Working Group, http://lepsusy.web.cern.ch/lepsusy/www/inos_moriond01/charginos_pub.html.
[9] K. L. Chan, U. Chattopadhyay, and P. Nath, Phys. Rev. D **58**, 096004 (1998).
[10] J. L. Feng, K. T. Matchev, and T. Moroi, Phys. Rev. Lett. **84**, 2322 (2000); Phys. Rev. D **61**, 075005 (2000); see also H. Baer, C. H. Chen, F. Paige, and X. Tata, Phys. Rev. D **52**,

2746 (1995); **53**, 6241 (1996); for a model-independent approach, see H. Baer, T. Krupovnickas, S. Profumo, and P. Ullio, J. High Energy Phys. 10 (2005) 020; J. L. Feng, K. T. Matchev, and D. Sanford, Phys. Rev. D **85**, 075007 (2012).
[11] J. L. Feng and D. Sanford, Phys. Rev. D **86**, 055015 (2012).
[12] R. Kitano and Y. Nomura, Phys. Lett. B **631**, 58 (2005); Phys. Rev. D **73**, 095004 (2006).
[13] N. Arkani-Hamed, Proceedings of the WG2 Meeting, Geneva, https://indico.cern.ch/conferenceOtherViews.py?view=standard&confId=157244.
[14] M. Papucci, J. T. Ruderman, and A. Weiler, J. High Energy Phys. 09 (2012) 035; C. Brust, A. Katz, S. Lawrence, and R. Sundrum, J. High Energy Phys. 03 (2012) 103; R. Essig, E. Izaguirre, J. Kaplan, and J. G. Wacker, J. High Energy Phys. 01 (2012) 074.
[15] H. Baer, V. Barger, P. Huang, and X. Tata, J. High Energy Phys. 05 (2012) 109.
[16] H. Baer, V. Barger, P. Huang, A. Mustafayev, and X. Tata, Phys. Rev. Lett. **109**, 161802 (2012); arXiv:1212.2655.
[17] H. Baer, V. Barger, and A. Mustafayev, J. High Energy Phys. 05 (2012) 091.
[18] L. Hall, D. Pinner, and J. T. Ruderman, J. High Energy Phys. 04 (2012) 131; S. P. Martin, Phys. Rev. D **81**, 035004 (2010); **82**, 055019 (2010); K. J. Bae, T. H. Jung, and H. D. Kim, Phys. Rev. D **87**, 015014 (2013).
[19] H. Baer, A. Lessa, S. Rajagopalan, and W. Sreethawong, J. Cosmol. Astropart. Phys. 06 (2011) 031.
[20] H. Baer, V. Barger, and P. Huang, J. High Energy Phys. 11 (2011) 031.
[21] J. Ellis, K. Olive, and Y. Santoso, Phys. Lett. B **539**, 107 (2002); J. Ellis, T. Falk, K. Olive, and Y. Santoso, Nucl. Phys. B652, 259 (2003); H. Baer, A. Mustafayev, S. Profumo, A. Belyaev, and X. Tata, J. High Energy Phys. 07 (2005) 065, and references therein.
[22] H. Baer, V. Barger, and A. Mustafayev, Phys. Rev. D **85**, 075010 (2012).
[23] H. Baer, F. Paige, S. Protopopescu, and X. Tata, arXiv:hep-ph/0312045.
[24] W. Beenakker, R. Hopker, and M. Spira, arXiv:hep-ph/9611232.
[25] H. Baer, V. Barger, S. Kraml, A. Lessa, W. Sreethawong, and X. Tata, J. High Energy Phys. 03 (2012) 092.
[26] V. D. Barger, W.-Y. Keung, and R. J. N. Phillips, Phys. Rev. Lett. **55**, 166 (1985); R. M. Barnett, J. F. Gunion, and H. E. Haber, Phys. Rev. D **37**, 1892 (1988); Phys. Lett. B **315**, 349 (1993); H. Baer, V. D. Barger, D. Karatas, and X. Tata, Phys. Rev. D **36**, 96 (1987); H. Baer, X. Tata, and J. Woodside, Report No. FSU-HEP-881011; Phys. Rev. D **41**, 906 (1990).
[27] See J. Gaunt, C-H. Kom, A. Kulesza, and W. J. Stirling, Eur. Phys. J. C **69**, 53 (2010) for a recent assessment of dileptons from SS W production and other SM sources at the LHC.
[28] M. V. Garzelli, A. Kardos, C. G. Papadopoulos, and Z. Trocsanyi, J. High Energy Phys. 11 (2012) 056.
[29] H. Baer, V. Barger, A. Lessa, and X. Tata, J. High Energy Phys. 09 (2009) 063.
[30] H. Baer, V. Barger, A. Lessa, and X. Tata, Phys. Rev. D **86**, 117701 (2012).
[31] S. Chatrchyan *et al.* (CMS Collaboration), Phys. Rev. Lett. **109**, 071803 (2012); arXiv:1212.6194.
[32] ATLAS Collaboration, Report No. ATLAS-CONF-2012-105.